ENGINEERING TRANSACTIONS • *Engng. Trans.* • **56**, 2, 101–116, 2008
Polish Academy of Sciences • Institute of Fundamental Technological Research

RIGID BODY ASSEMBLY IMPACT MODELS FOR ADIABATIC CUTOFF EQUIPMENTS

M. Massenzio, S. Pashah, E. Jacquelin, A. Bennani

Université de Lyon, Lyon, F-69003, France
Université Lyon 1, UMRT9406, LBMC, IUT B
Département Génie Mécanique et Productique
Villeurbanne, F-69627, France

This paper is concerned with systems consisting of components colliding with each other. In particular, a high velocity adiabatic impact cutoff machine is investigated. For general understanding of the impact dynamics (affected by a large number of parameters), the mechanisms are modelled in a simplified and accurate manner. Two simple models are developed: the energy-balance model and the spring-mass model. The energy-balance model is based on the principle of total energy conservation. It provides only the punch minimum kinetic energy required for efficient cutting. Concerning the spring-mass model, the different components are represented by rigid masses and their deformations are modelled by springs (linear or non-linear in the case of contact stiffness). The resulting non-linear equations are solved using the Newmark numerical technique. The impact force, velocity, displacement and acceleration histories are calculated what makes possible a fine description of the cutoff cycle steps. The two models are helpful for both the design and tuning of the mechanisms involving impacts between their components.

Key words: impact, rigid body, adiabatic cutoff, spring-mass model, energy-balance model.

1. Introduction

A wide variety of engineering applications concern components colliding with each other. This is particularly the case in mechanisms including clearances or gaps. In most cases the principle of operation is based on repeated impacts: impact hammers, high velocity adiabatic impact cutoff, blanking or powder compaction machines, impact-forming machines, etc. On the other hand, impacts may be unwanted because they may prove to be harmful to the reliability of the equipment: rotors with bearing clearance, gears, wheel-rail interaction of high-speed trains, etc. The theoretical models presented in this paper are concerned with high-velocity adiabatic impact cutoff machines. Although similar to conventional presses, high-velocity adiabatic impact presses use high-speed punch motion to carry out the cutting operation. The tool velocity is generally between

10 m/s to almost 100 m/s, whereas in the case of conventional presses, the velocity is about 0.3 m/s and a static approach is satisfactory. When sufficient kinetic energy is imparted to the cutting tool, the material being cut cannot dissipate heat fast enough. The temperature increases adiabatically due to the extremely short time and energy concentration in the local area identified as the "adiabatic zone" [2–4, 7, 10, 11, 14]. The material softens instantly (adiabatic softening) and the moving die separates the material into two parts. The main benefits of adiabatic cutting are high quality end cuts, tight length or volume tolerances, square ends and high production rates. However, the key factor in the success of this technology depends both on creating sufficient energy to reliably reproduce the adiabatic softening phenomenon and on controlling the required energy. The former is a matter of technology, but the latter is associated with complex dynamic phenomena and is of interest for researchers [8]. The process exhibits a cutting tool thrusted by a ram. A clearance allows the tool to accelerate and reach the required velocity before hitting the material. The adiabatic softening completes the cut-off and a die base is needed to stop the tool. This process involves a large number of impacts between the various components of the machine.

Each machine component can be modelled as a nearly rigid body. The phenomena linked to two colliding bodies have been widely studied in the literature [13]. Impact initiates when two bodies move close to each other with relative velocity. The incidence occurs when a single contact point appears on the surface of each body. After incidence, the contact pressure in the small contact area prevents the interpenetration of the bodies. During the impact, the pressure in the contact area produces local deformations and indentations, and has a resultant action that acts on the colliding bodies in opposite directions. Initially, the force increases with increasing indentation and it reduces the relative velocity at which the bodies move close to each other. After a time, the work done by the contact force is sufficient to bring the relative velocity to zero. Subsequently, the elastic energy stored during compression drives the two bodies apart until finally they separate with a acertain relative velocity. As regards the impact between solid bodies, the contact force which acts during the collision, is the result of local deformations that are required for the surfaces of the two bodies to conform in the contact area. The local deformations can be elastic or plastic and vary according to the relative incident velocity and to the hardness of the colliding bodies. In addition to local deformations, there are also global deformations of the bodies. These global deformations mainly depend on the impact velocity, the mass ratio, the boundary conditions and the geometry of the bodies. The physical process during impact is strongly non-linear and discontinuous. A fine numerical analysis of the system is an alternative to tackle the problem (i.e. the finite – elements model). But, it is difficult to understand the phenomena

and to identify the leading parameters, which are required for the fine tuning of the machine. Some simplified models are available in the literature to study impact dynamics. Generally, the models are classified according to the dynamic response of the structure: impact on a half-space, quasi-static approach and complete models [13]. With the first two approaches, energy balance models can be used to predict the maximum contact force and the contact duration [1, 12]. However, the energy balance model is restricted to two free bodies with no external forces. It is not suitable to multi-body impact, and to the impact with an external force applied to the bodies.

In order to enable the design and fine tuning of the high velocity adiabatic impact cutoff machines, appropriate models need to be developed. The objective of this article is to study two models available to analyze the multi-impact dynamics: the energy balance model and the spring-mass model. Section 2 presents the analytical and numerical aspects of the spring-mass model developed for the purpose of the study. An example of a high velocity adiabatic impact cutoff machine is presented in Sec. 3. Sections 3.2 and 3.3 deal with the spring-mass and the energy-balance model results respectively. The two analyses are compared with each other and the relevances of each model are discussed.

2. Spring-mass model

2.1. Equations of motion

A general spring-mass model with n degrees of freedom is considered as shown in Fig. 1. The springs are non-linear and the behaviour law is written as:

$$P = k \cdot x^p \tag{2.1}$$

where P is the spring force, k is the contact stiffness parameter and p depends on the non-linear effect.

Considering a particular mass "i", the equation of motion is defined as the non-linear differential equation (Fig. 2):

$$\begin{aligned} &m_i \cdot \ddot{x}_i + \lambda_1 \cdot k_i \cdot |x_i - x_{i-1}|^{p_i} + c_i \cdot (\dot{x}_i - \dot{x}_{i-1}) \\ &\qquad +\lambda_2 \cdot k_{i+1} \cdot |x_i - x_{i+1}|^{p_{i+1}} + c_{i+1} \cdot (\dot{x}_i - \dot{x}_{i+1}) = F_i \\ &\text{where} \\ &\lambda_1 = 1 \quad \text{for } x_i > x_{i-1} \quad \text{else } -1 \\ &\lambda_2 = 1 \quad \text{for } x_i > x_{i+1} \quad \text{else } -1, \end{aligned} \tag{2.2}$$

which may be expressed as

$$[m] \cdot [\ddot{x}] + [c] \cdot [\dot{x}] + [P(x)] = [F] \tag{2.3}$$

for the complete system, where the mass matrix $[m]$ and the viscous damping matrix $[c]$ are given by:

$$[m] = \begin{bmatrix} m_1 & 0 & \dots & 0 \\ 0 & m_2 & & \vdots \\ \vdots & & \ddots & \\ 0 & \dots & & m_n \end{bmatrix},$$

(2.4)

$$[c] = \begin{bmatrix} c_1 + c_2 & -c_2 & 0 & \dots & 0 \\ -c_2 & c_2 + c_3 & -c_3 & & \vdots \\ 0 & -c_3 & \ddots & & \\ \vdots & & & & \\ 0 & \dots & 0 & -c_n & c_n + c_{n+1} \end{bmatrix}.$$

$[P(x)]$ is the non-linear forces vector and it is given by:

(2.5)

$$[P(x)] = \begin{bmatrix} k_1 \cdot x_1^{p_1} + k_1 \cdot (x_1 - x_2)^{p_2} \\ k_2 \cdot (x_2 - x_1)^{p_2} + k_3 \cdot (x_2 - x_3)^{p_3} \\ \vdots \\ k_n \cdot (x_n - x_{n-1})^{p_n} + k_{n+1} \cdot x_n^{p_{n+1}} \end{bmatrix}.$$

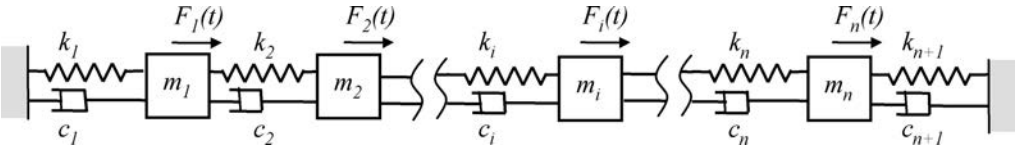

FIG. 1. Non-linear spring-mass system with n degrees of freedom.

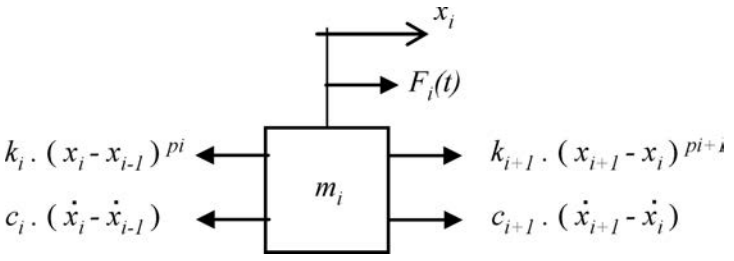

FIG. 2. Notation for the mass "*i*".

The velocity vector $[\dot{x}]$, acceleration vector $[\ddot{x}]$ and external forces vector $[F]$ are defined as:

$$[\dot{x}] = \begin{bmatrix} \dot{x}_1(t) \\ \dot{x}_2(t) \\ \vdots \\ \dot{x}_n(t) \end{bmatrix}, \qquad [\ddot{x}] = \begin{bmatrix} \ddot{x}_1(t) \\ \ddot{x}_2(t) \\ \vdots \\ \ddot{x}_n(t) \end{bmatrix}, \qquad [F] = \begin{bmatrix} F_1(t) \\ F_2(t) \\ \vdots \\ F_n(t) \end{bmatrix}. \tag{2.6}$$

2.2. Numerical integration

The Newmark numerical technique [9] is used to calculate the displacement vector $[x]$ from Eq. (2.3). First, the time duration of impact T is subdivided into q equal steps $\triangle t$, so that $\triangle t = T/q$. Considering that the displacement vector (x_i), the velocity vector $(\dot{x}_i)$ and the acceleration vector $(\ddot{x}_i)$ are known for time step $(t_i = i \cdot \triangle t)$, the method uses an approximation to calculate the value of the three vectors at the time step t_{i+1}. The non-linear equations of motion have to be linearized in order to suit the method. Assuming that the solution is known at time step t_i, the equation at time step t_{i+1} is given by:

$$[m] \cdot [\ddot{x}_{i+1}] + [c] \cdot [\dot{x}_{i+1}] + [P(x_{i+1})] = [F_{i+1}] \tag{2.7}$$

$[P(x_{i+1})]$ is expressed as:

$$[P(x_{i+1})] = [P(x_i)] + [K_i] \cdot [\triangle x_i] \tag{2.8}$$

where $[\triangle x_i] = [x_{i+1}] - [x_i]$ and $[K_i]$ is the stiffness tangent matrix at time step t_i. Equation (2.7) and Eq. (2.8) give:

$$[m] \cdot [\ddot{x}_{i+1}] + [c] \cdot [\dot{x}_{i+1}] + [K_i] \cdot [x_{i+1}] = [\overline{F}_{i+1}] \tag{2.9}$$

with

$$[\overline{F}_{i+1}] = [F_{i+1}] - [P(x_i)] + [K_i] \cdot [x_i]. \tag{2.10}$$

Since the right-hand side of Eq. (2.10) is completely known, this equation can be solved for x_{i+1}, using the Newmark method. The x_{i+1} found is only an approximate vector, due to the linearization process used in Eq. (2.10). To improve the accuracy of the solution and to avoid the development of numerical instabilities, an iterative process can be used within the current time step (e.g. Newton Raphson).

For the linearization approximation of Eq. (2.10), the tangent matrix stiffness is calculated. This is obtained by differentiating the vector of non-linear forces $[P(x)]$ with respect to the displacement vector $[x]$, i.e.:

$$[K] = \frac{\partial}{\partial [x]} [P(x)]. \tag{2.11}$$

From Eq. (2.5), one obtains:

$$
(2.12)\qquad [K] = \begin{bmatrix}
\begin{pmatrix} p_1\, k_1\, x_1^{p_1-1} \\ +\, p_2\, k_1\, (x_1 - x_2)^{p_2-1} \end{pmatrix} & \begin{pmatrix} -p_2\, k_1\, (x_1 - x_2)^{p_2-1} \end{pmatrix} & & \\
\begin{pmatrix} -p_2\, k_1\, (x_1 - x_2)^{p_2-1} \end{pmatrix} & \begin{pmatrix} p_2\, k_2\, (x_2 - x_1)^{p_2-1} \\ +\, p_3\, k_3\, (x_2 - x_3)^{p_3-1} \end{pmatrix} & & \\
\vdots & & & \\
0 & \cdots & \cdots & 0 \\
 & & & \vdots \\
 & & \ddots & \\
 & & & \begin{pmatrix} p_n\, k_n\, (x_n - x_{n-1})^{p_n-1} \\ +\, p_{n+1}\, k_{n+1}\, x_n^{p_n} \end{pmatrix}
\end{bmatrix}.
$$

3. Modelling of a simplified cutting machine

3.1. The model

Figure 3 (left) shows the simplified adiabatic cutting machine to be modelled (i.e. only the main parts of the actual machine are taken into account). The metal sheet lies on the cutting-off die which is assumed to be linked to the inertia reference frame, i.e. the suspension is not considered. The punch is moved by a hydraulic actuator (cylinder is not represented). Figure 4 a shows the cylinder force. The force is initially zero. It becomes constant for 0.1 s (37 000 N) and eventually returns to zero. A Haversine function is used to represent the smooth transitions between zero and 37 000 N. The transition duration is 2 ms. After the cutting phase, the punch is stopped by the die base. The spring-mass model associated is shown in Fig. 3 (right). The punch and the die base are represented by two rigid masses m_1 and m_2 respectively. The two masses are connected through a Hertzian spring that represents the contact load-deformation characteristics and the initial gap (K_{12}) [15], and the die base is attached to the reference frame through a linear spring (K_{22}). The metal sheet is represented by the relationship between the force and the displacement [5, 6] including the

material's properties, the thickness and the cutting perimeter of the sheet. This relationship and the initial gap are represented by the non-linear stiffness K_{11}, given in Fig. 4 b (with no gap). The initial gap of spring K_{11} is one of the tuning parameters of the machine. The distance between the punch and the metal sheet enables the punch to reach the required cutting velocity. The initial gap of spring K_{12} is the sum of the initial gap of spring K_{11}, of the metal sheet thickness and of a supplementary gap to assure that the metal sheet is completely cut before the punch impacts the die base. Numerical values of mass and stiffness are given in Table 1.

The numerical integration is performed as presented in Sec. 2.2, with a time step of 10^{-5} s and a time duration of 0.2 s. Four different initial gaps between the punch and the metal sheet are tested : no gap, 9 mm, 10 mm and 43 mm.

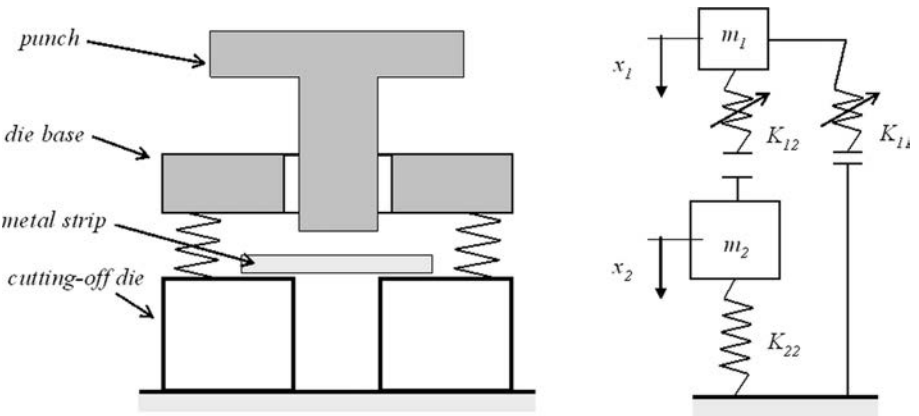

FIG. 3. The model (left: the simplified machine, right: the spring-mass model).

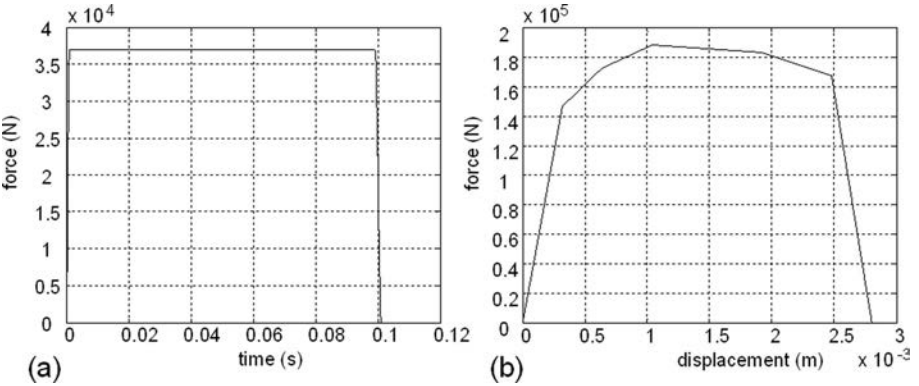

FIG. 4. Force applied to the punch (a); relationship between the force and the displacement (b).

Table 1. Numerical data of the two-degrees-of-freedom model.

Mass		Stiffness	
m_1	40 kg	K_{11}	initial gap – 4 values tested: 0, 9, 10 & 43 mm & cutting force-displacement relationship (Fig. 4 b)
m_2	100 kg	K_{12}	initial gap = initial gap of K_{11} + metal sheet thickness (2.8 mm) + supplementary gap (0.2 mm) & contact law : $P = 10^{13} \cdot x^{2,2}$ (x is the indentation)
		K_{22}	2.10^8 N/m

3.2. The spring-mass model

Figures 5, 6 and 7 show the punch and the die base displacement, velocity and acceleration history respectively, for the four initial gaps (0, 9, 10 & 43 mm). On a single plot, Fig. 8 shows the punch displacement relative to the metal sheet (synthesis of the above results). Figure 9 shows the force history between the punch and the metal sheet.

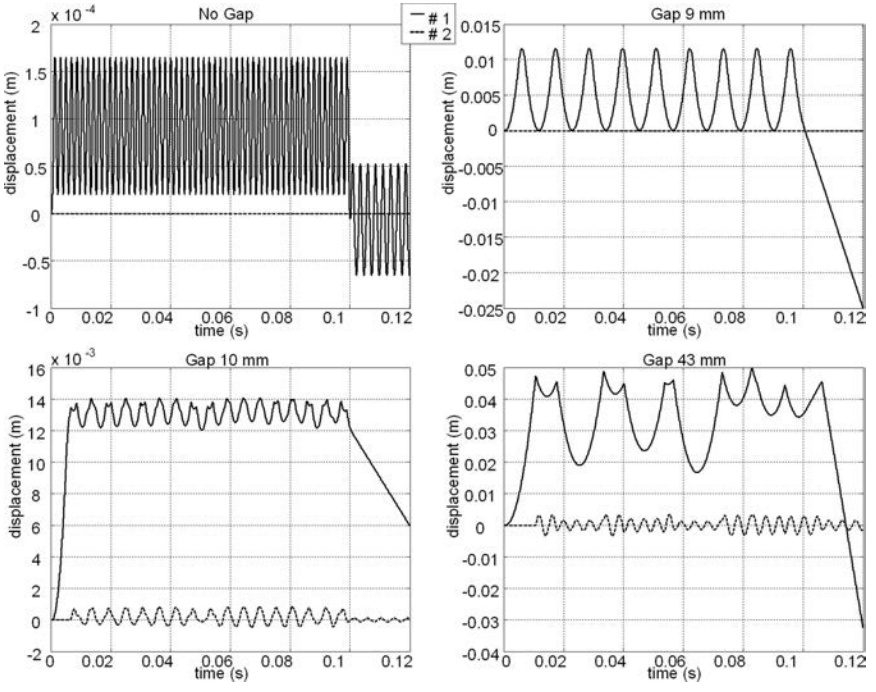

FIG. 5. The displacement history (no gap – gap 9 mm – gap 10 mm – gap 43 mm).

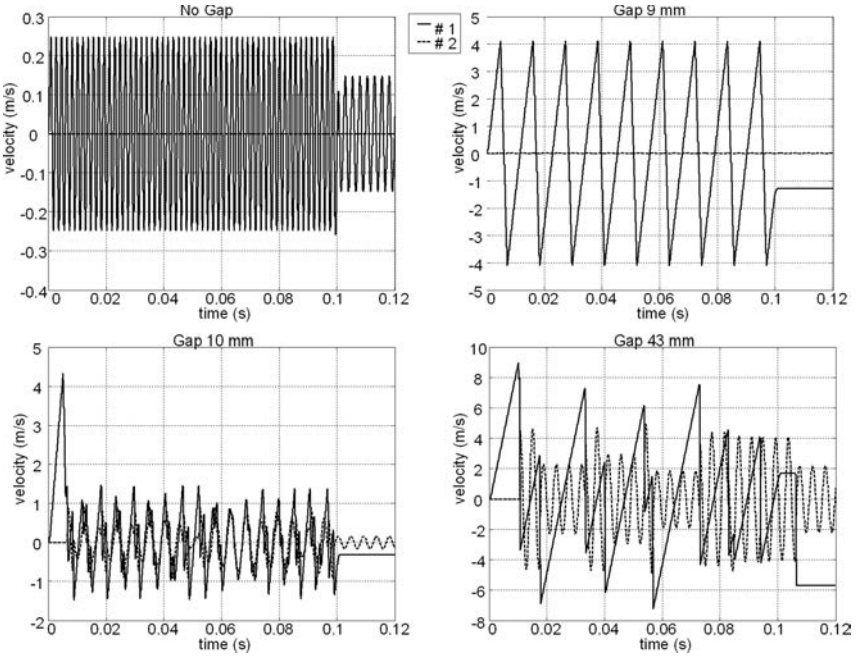

FIG. 6. The velocity history (no gap – gap 9 mm – gap 10 mm – gap 43 mm).

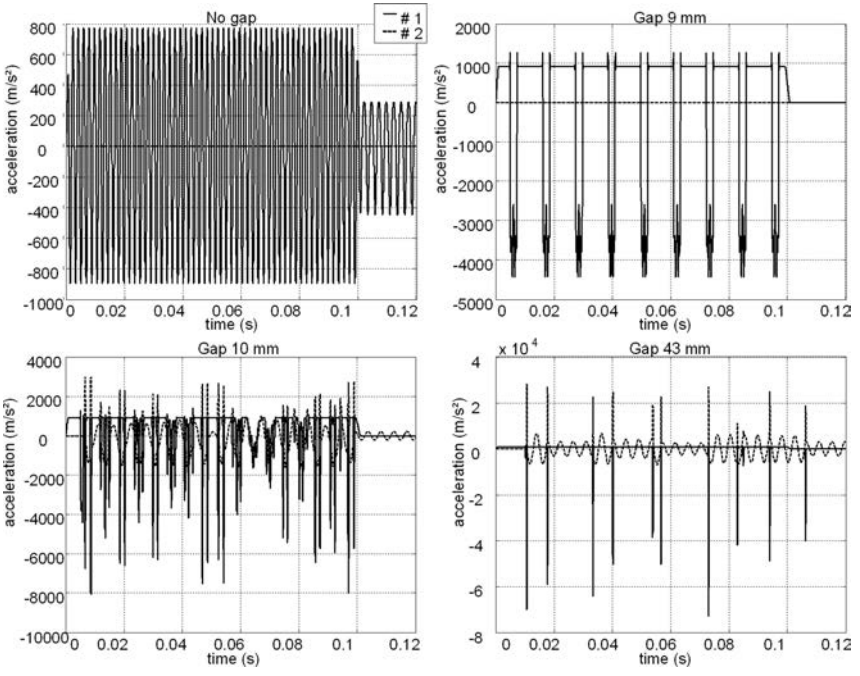

FIG. 7. The acceleration history (no gap – gap 9 mm – gap 10 mm – gap 43 mm).

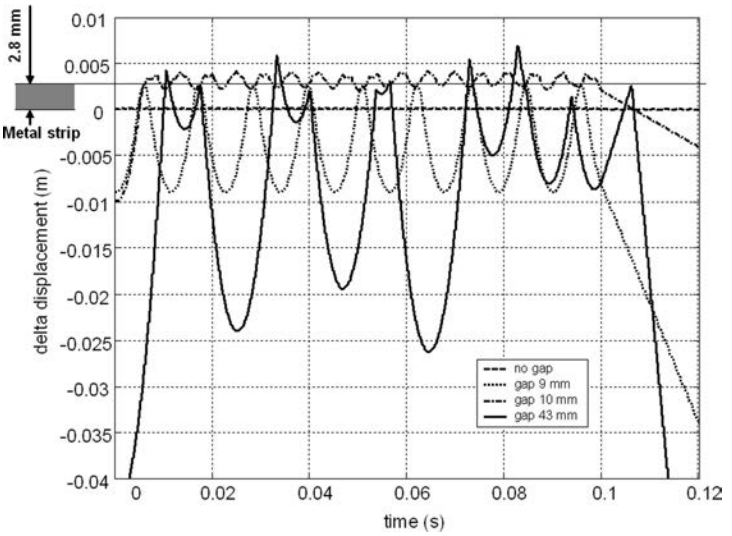

FIG. 8. The displacement relative to the metal sheet (no gap – gap 9 mm – gap 10 mm – gap 43 mm).

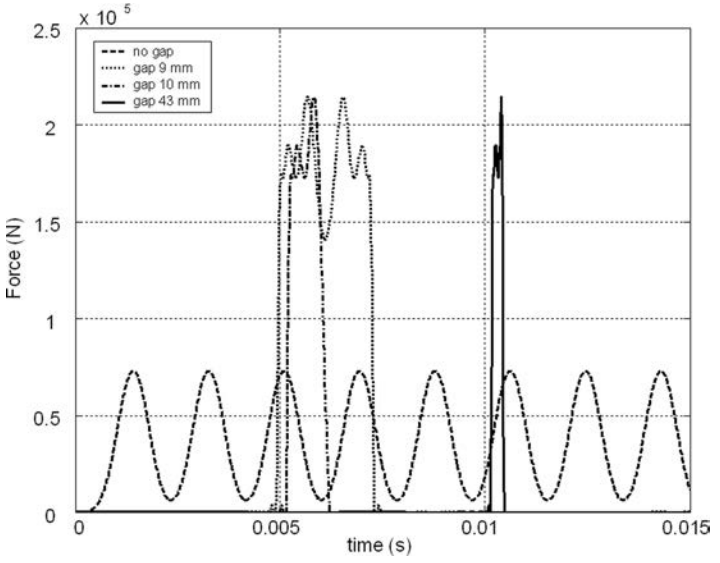

FIG. 9. The force history (no gap – gap 9 mm – gap 10 mm – gap 43 mm).

The results with no gap are typical of a system with one degree of freedom with Heaviside excitation (the punch is the mass and the metal sheet is the spring). The displacements are very small: between -0.204 mm and 0.164 mm within the range $0 - 0.1$ s. This means that the metal sheet is slightly indented.

After 0.1 s (*i.e.* no more ram force), the response oscillates between −0.065 mm and 0.052 mm, corresponding to the free vibrations of a one-degree-of-freedom system. With an indentation below 0.320 mm, the relationship between the force and the displacement is linear (Fig. 4 b). The corresponding stiffness is $K_{11} = 4.58.10^8$ N/m. The eigenfrequency of the one-degree-of-freedom system can be expressed as:

$$f = \frac{1}{2\pi}\sqrt{\frac{K_{11}}{m_1}} \tag{3.1}$$

leading to the value of 538 Hz. In Fig. 5, the 53.5 oscillations within the range $0-0.1$ s lead to the same eigenfrequency value. The velocity of the punch is also limited to very small values (less than 0.25 m/s), so as the acceleration (less than 900 m/s^2). Both results show that the dynamic effects are insignificant in the no-gap case. Furthermore, there is no loss of contact as shown by the harmonic behaviour of the acceleration. As the metal sheet is not cut, the die base remains at rest. Note that the model does not take into account the effect of repeated damage on the metal sheet, whereas the actual cutting process can lead to final cutting. Anyway, the adiabatic cutting process is efficient only if the first impact leads to complete cutting. If not, the quality of the surface condition is of no interest. The present model is not devised to take these effects into account.

With a gap of 9 mm, the metal sheet is not cut either. Figure 5 shows a maximum displacement of 11.5 mm. The indentation of the metal sheet is then 2.5 mm (lower than the thickness 2.8 mm, Fig. 8). In comparison with the case with no gap the mechanisms are different. The amplitude of the velocity and acceleration are higher: the maximum velocity is 4.09 m/s, and the maximum acceleration is 4426 m/s^2. Consequently, in Fig. 6 and 7 one can observe successive rebounds of the punch on the metal sheet.

The metal sheet is cut with an initial gap of 10 mm, as shown in Fig. 5. During the first impact, the displacement reached the value of 13.4 mm, corresponding to an "indentation" of 3.4 mm – larger than the thickness: 2.8 mm (Fig. 8). After the cutoff, the punch is stopped by the die base, and several punch impacts on the die base are observed until the external force returns to zero (0.1 s). Then, the punch has a uniform movement and the die base oscillates such as a one-degree-of-freedom system. Hence, the minimum velocity for the cutoff is 4.32 m/s. With a gap of 43 mm, the cutoff is similar to the latter case, with higher values for the displacement, velocity and acceleration.

Focusing only on the results for the initial gap of 43 mm, the cutting work can be divided into 4 steps as shown in Fig. 10.

- Step #1 is the acceleration of the punch. The leading parameters of this step are the cylinder force, the initial gap and the mass of the punch (m_1)

(Fig. 10 – 1). After 10 ms of free run, the punch impacts the metal sheet (Fig. 10 – 2 start).

- Step #2 is the cutting of the metal sheet, both influenced by the cylinder force (which is still active) and by the initial velocity (8.93 m/s). The duration of cutting is 0.33 ms (whereas it is about 3 ms with a conventional press). At the end of step #2 (Fig. 10 – 2 end), the punch velocity is still high: (7.9 m/s). During this step, the maximum acceleration of the punch is 4424 m/s^2, equal to the difference between the acceleration of the punch (37000/40 = 925 m/s^2) and the resistance force of the metal sheet (Fig. 4 b).
- Step #3 starts just after cutting as the punch impacts the die base (Fig. 10 – 3). Oscillations of the punch are due to successive rebounds on the die base under the action of the cylinder. These successive shocks induce free oscillations of the die base (behaving as a one-degree-of-freedom system). As the velocity of the punch is still high, the accelerations of the punch can reach very high values (73000 m/s^2); this result is of importance for the actual machine parts design). Step #3 lasts until the cylinder stops acting on the punch.
- In step #4, the free oscillations of the die base have to be treated by specific dampers. The uniform movement of the punch has to be clamped for the next cutting (Fig. 10 – 4). This step is of no interest for the present study and the results are not discussed in this paper.

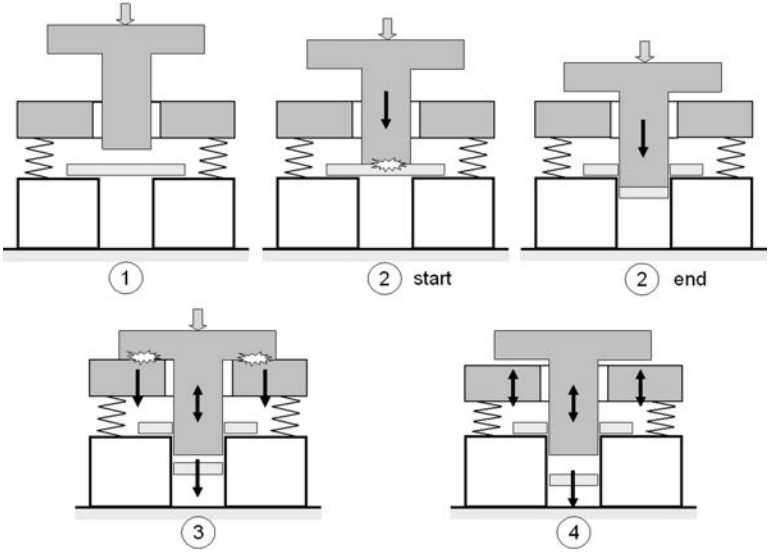

Fig. 10. The 4 steps of cutting.

It is clear from Fig. 8 that the minimum initial gap required for the cutting is 10 mm. In the no-gap case, step #1 is not possible and therefore there is no kinetic energy stored before contact for the cutting. The force of the punch on the metal sheet reaches the maximum value of 72 800 N (Fig. 9), which is higher than the force produced by the rams (37 000 N) due to dynamic effects, but less than the maximum force required for cutting (Fig. 4 b). The maximum forces for the three different gaps: 9 mm, 10 mm, 43 mm are approximately the same: 214 000 N. This is higher than the maximum force from the cutting relationship between the force and the displacement: 189 00 N (Fig. 4 b). Yet, with a 9 mm gap, the kinetic energy stored during step #1 is not sufficient and therefore step #2 is not fully completed.

Table 2. Results for the four gaps (spring-mass model).

Gap (mm)	Cutting?	before cutting (step #1)		during cutting (step #2)	
		Velocity (m/s)	Kinetic energy (J)	duration (ms)	Max acceleration (m/s^2)
0	no	0	0	–	896 (oscillations)
9	no	4.09	335	–	4426 (rebounds)
10	yes	4.32	373	1.07	8043
43	yes	8.93	1594	0.33	69800

Table 2 shows a synthesis of the main data required to analyze the cutting: velocity before impact and the corresponding kinetic energy, cutting duration and maximum acceleration of the punch. The data will be compared to the results from the energy-balance model as follows.

3.3. The energy-balance model

The force of the cylinder acting on the punch is 37 000 N. In the case of a static process (conventional press), the force required for cutting of the metal sheet is at least $1.89\ 10^5$ N (see relationship between the force and the displacement in Fig. 4 b). It is then the kinetic energy stored by the punch during the step #1 that controls the cutting.

The energy-balance model is based on the principle of conservation of total energy of the punch-metal sheet system. Assuming that the structure behaves quasi-statically, the kinetic energy of the impacting punch ($E_{\text{cin}} = \frac{1}{2}.m_1.v_1^2$ at the end of step #1) is equated to the energy required for the metal sheet cutting (E_{cut} – step #2):

$$E_{\text{cin}} = E_{\text{cut}}. \tag{3.2}$$

The constant force of the ram on the punch, essential during the step #1, is neglected during impact (step #2). Moreover, the energy losses from friction between parts, material damping and vibrations are neglected.

The required cutting energy (step #2) is the integral of the product of the force acting on the metal sheet (F_{cut}) and the deformation (x):

$$E_{\text{cut}} = \int_0^e F_{\text{cut}}.\mathrm{d}x, \tag{3.3}$$

where e is the thickness of the metal sheet, and F_{cut} is derived from the relationship between the force and the displacement (Fig. 4 b). For the present case, $E_{\text{cut}} = 436$ J.

During step #1, Newton's second law of motion applied to the punch led to:

$$F = m_1.\gamma_1, \tag{3.4}$$

where F is the ram's force that can be considered constant, and γ_1 is the punch acceleration. From Eq. (3.4) the punch acceleration is constant and equal to 925 m/s^2. As the initial velocity and displacement are zero, one can obtain the velocity and displacement functions:

$$v_1 = \gamma_1 \cdot t, \tag{3.5}$$

$$x_1 = \frac{1}{2} \cdot \gamma_1 \cdot t^2. \tag{3.6}$$

From Eq. (3.6), equating the displacement to the initial gap, one can solve the time of impact and consequently, the velocity and the kinetic energy before impact. The results (Table 3) agree with the spring-mass model (Table 2 – note that only the acceleration step #1 is concerned). Comparing the kinetic energy before impact and the result of Eq. (3.3): $E_{\text{cut}} = 436$ J, the energy-balance model does not predict complete cutoff with a 10 mm gap.

Table 3. Results for the four gaps (energy-balance model).

Gap (mm)	Acceleration (m/s^2)	Time of impact (ms)	Impact velocity (m/s)	Kinetic energy (J)
0	925	0	0	0
9	925	4.41	4.08	333
10	925	4.65	4.30	370
43	925	9.64	8.92	1591

Equating the minimum kinetic energy with the cutting energy from Eq. (3.3), the minimum impact velocity for cutting is:

$$v_1 = \sqrt{\frac{2.E_{\text{cut}}}{m_1}} \tag{3.7}$$

which gives a velocity of 4.67 m/s. With Eqs. (3.4), (3.5) and (3.6), the minimum gap (x_{gap}) is:

$$x_{\text{gap}} = \frac{E_{\text{cut}}}{F} \tag{3.8}$$

which gives a minimum gap of 11.8 mm. The minimum gap calculated by means of the energy-balance model agrees reasonably well with the results from the spring-mass model (minimum gap between 9 to 10 mm – Table 2).

4. Conclusions

This paper has presented two simple models, the energy-balance model and the spring-mass model, to describe the dynamics of mechanisms involving clearances or gap and featuring repeated impacts. Both models are applied to a high velocity adiabatic impact cutoff machine. The energy-balance model is based on the principle of total energy conservation: the impacting component kinetic energy is equated to the impacted component deformation energy. The spring-mass model uses the assumption that the components are rigid enough to be modelled by masses, and that the masses are connected by linear or non-linear springs. Both models include contact stiffness between the components by the use of non-linear springs.

The energy-balance model is able to predict the minimum kinetic energy required for the metal sheet cutoff. The model is simple for use, and the results provided are useful for tuning of one essential parameter of the machine: the value of the initial gap between the punch and the metal sheet. However, the model is limited to systems with only two components.

The development of the spring-mass model is more complex, and particularly a numerical integration of displacements is needed (Newmark numerical technique). Unlike the energy-balance model, it can be applied to systems with more than two components. The minimum kinetic energy calculated with the energy-balance model agrees reasonably well with the spring-mass model prediction. Moreover, the spring-mass model predicts the displacement, the velocity, the acceleration and the contact force history for each mass. Accurate analysis of the cutoff process shows that the kinetic energy of the punch before impact is the leading parameter, and that the force of the ram has a small influence during the cutoff. This fact can explain accurately why the energy-balance is efficient.

The two models presented in this paper can be applied to other vibratory machinery and equipment, featuring multi-degree-of-freedom oscillators with colliding components.

References

1. S. Abrate, *Modeling of impacts on composite structures*, Composite structures, **51**, 2, 129–138, 2001.
2. A.-S. Bonnet-Lebouvier, A. Molinari and P. Lipinski, *Analysis of the dynamic propagation of adiabatic shear bands*, International Journal of Solids and Structures, **39**, 16, 4249–4269, 2002.
3. T. J. Burns and M. A. Davies, *On repeated adiabatic shear band formation during high-speed machining*, International Journal of Plasticity, **18**, 1, 487–506, 2002.
4. X. W. Chen, Q. M. Li and S. C. Fan, *Initiation of adiabatic shear failure in a clamped circular plate struck by a blunt projectile*, International Journal of Impact Engineering, **31**, 7, 877–893, 2005.
5. A. Eberle, D. Klingbeil and J. Schicker, *The calculation of dynamic j_R-curves from the finite element analysis of a Charpy test using a rate-dependent damage model*, Nuclear Engineering and Design, **198**, 1–2, 75–87, 2000.
6. A. L. Gurson, *Continuum theory of ductile rupture by void nucleation and growth: Part I, yield criteria and flow rules for porous media*, Journal of Engineering Materials and Technology, **99**, 2–15, 1977.
7. J. R. Klepaczko, *Review on critical impact velocities in tension and shear*, International Journal of Impact Engineering, **32**, 1–4, 188–209, 2005.
8. G. W. Luo, *Dynamics of an impact-forming machine*, International Journal of Mechanical Sciences, **48**, 11, 1295–1313, 2006.
9. S. S. Rao, *Mechanical vibrations*, Second edition, Addison-Wesley Publishing Company, 1990.
10. K. M. Roessig and J. J. Mason, *Adiabatic shear localization in the dynamic punch test, part I: experimental investigation*, International Journal of Plasticity, **15**, 3, 241–262, 1999.
11. K. M. Roessig and J. J. Mason, *Adiabatic shear localization in the dynamic punch test, part II: numerical simulations*, International Journal of Plasticity, **15**, 3, 263–283, 1999.
12. K. N. Shivakumar, W. Elber and W. Illg, *Prediction of impact force and duration due to low velocity impact on circular composite laminates*, ASME, **52**, 674–680, 1985.
13. W. J. Stronge, *Impact Mechanics*, Cambridge University Press, Cambridge 2000.
14. X. Teng, T. Wierzbicki and H. Couque, *On the transition from adiabatic shear bending to fracture*, Mechanics of Materials, **39**, 2, 107–125, 2007.
15. S. Timoshenko and N. Goodier, *Theory of elasticity, 3rd edition*, McGraw-Hill, New-York 1970.

Received February 14, 2007; revised version October 2, 2007.